Sandwich atomic structure in tetrahedral amorphous carbon: Evidence of subplantation model for film growth from hyperthermal species

J. P. Zhao* and Z. Y. Chen

Ion Beam Laboratory, Shanghai Institute of Metallurgy, Chinese Academy of Sciences, Shanghai 200050, People's Republic of China and Shikoku National Industrial Research Institute, Takamatsu 761-0395, Japan

(Received 1 June 2000; revised manuscript received 8 August 2000; published 1 March 2001)

High-resolution transmission electron microscopy (HRTEM) was used to characterize the cross-sectional and planar atomic structures and bonding states of highly tetrahedrally bonded amorphous carbon (ta-C) films, particularly concentrating on the surface layer and interface between substrate and pure ta-C film. A ''sandwich'' cross-sectional structure was found to be existing in ta-C grown from hyperthermal carbon species, and can be expressed as $A/B/A$ layer-by-layer stacks. The interface (A) was shown to be very thick ($\sim$40 nm), and consisted of sp^2-bonded carbon domains and quasicontinuous two-dimensional layers. The initial pure carbon layer on silicon substrate exhibits relatively ordered atomic configuration, which can be attributed to the presence of graphitelike structure. The surface layer (A) was investigated in detail by using both cross-sectional and planar HRTEM observations. Results indicated a large number of ordered structure existed in the surface, in the manner of entangled ribbons that were identified to be sp^2-bonded glassy carbon. The ordered sp^2-bonded surface layer is proposed to form immediately while stopping deposition, i.e., the final stage of film growth, due to thermal spike-induced stress relaxation on surface. The interior film (B) is predicted to possess higher sp^3-bond content than that measured by electron-energy-loss spectrum. In addition, slow positron annihilation, as well as a classical-trajectory calculation concerning the projected range R_p and range straggling ΔR_p of carbon species implantation into silicon substrate, were conducted for further investigating and interpreting the observed atomic structures in surface, interior film, and interface. The fact that sp^2-bonded surface and interface are present in a primarily sp^3-bonded film gives a direct corroboration of subplantation model and compressive stress mechanism for sp^3-bonded film growth from hyperthermal species.

DOI: 10.1103/PhysRevB.63.115318 PACS number(s): 68.35.−p, 68.55.−a, 61.43.Dq, 68.37.Lp

I. INTRODUCTION

It has been well established that the deposition of carbon using medium-energy ion beams can produce thin films with properties similar to those of crystalline diamond. The material has been shown to possess a high proportion of sp^3 C-C bonds (>80%),[1] and neutron scattering results yield a mean C-C bond length of 0.153 nm and a bond angle of $\sim$110°, consistent with a network dominated by tetrahedral bonding.[2] The material is therefore now called tetrahedral amorphous carbon (ta-C) to distinguish it structurally from other forms of carbon, in particular evaporated and sputtered a-C, which are dominant in sp^2 bonding. Nowadays, it is generally accepted that the mechanism promoting sp^3 bonding over the normally more stable trigonal planar (sp^2) structure for amorphous carbon is related to shallow subsurface implantation[3–7] of medium-energy [energies (E) $\approx 20-10^3$ eV] carbon species. The impinging species usually include pure or a mixture of ions, free radicals, and atomic cluster with enough energy and flux, and therefore are called as hyperthermal species in order to differentiate from thermal species with energy less than 10 eV. The best methods reported for depositing ta-C are mass-selected ion-beam[3] and filtered arc deposition (FAD).[5,8] In both cases, the optimal properties of ta-C, including sp^3 content, compressive stress, hardness, density, and refractive indexes are strongly interrelated, and almost invariably obtained within an energy interval of incident species which is practically the same for all parameters typical of diamondlike qualities. However, the energy window depends on the applied method and deposition conditions. Some of the values reported in the literature are $E=20-60$ eV,[5] 50–240 eV,[8,9] and 100–2000 eV.[10] Below and above these energy windows the amount of sp^2-bonded carbon atoms increases, and physical properties degrade correspondingly.

The role of hyperthermal species on the evolution of diamondlike phases has been subject to a number of experimental and theoretical studies. A decade ago, Lifshitz *et al.* introduced the subplantation (shallow subsurface implantation) model for film growth from hyperthermal species.[3,4] The subplantation process is basically divided into three stages with distinct time scales based on the hyperthermal species-target interactions, i.e., (i) a collisional stage in which the hyperthermal species transfers its energy to the target atoms ($\sim 10^{-13}$ sec) during penetration into subsurface; (ii) a thermalization stage where exited surrounding atoms reach thermal equilibrium with the energetic species due to collision cascade ($\sim 10^{-11}$ sec), and this process can be treated within the ''thermal spike'' concept;[11] (iii) a long-term relaxation stage ($\sim 10^{-10}-1$ sec), in which diffusion processes, chemical reactions, phase transformations, and stress relaxation processes take place, and the final structure of the material is determined. In this model, the physical quantities including projected range (R_p) of species, range straggling (ΔR_p), backscattering yield (Y_{BS}), sputtering yield (S), and damage (N_d) have been considered critical to the film growth. Generally, small R_p and ΔR_p (high local concentration), low S and Y_{BS}, and controlled N_d are necessary for high

sp^3-bonded carbon phase (diamondlike phase) formation. The preferential displacement also has been thought as a dominating mechanism for the formation of a diamondlike phase in subplantation model, especially in the energy range between 50–200 eV.[3] However, recent experimental data and theoretical studies indicate that displacement energy for diamondlike phase is less than 50 eV,[12,13] so the preferential displacement effect will be somewhat less pronounced. In the subplantation model of Lifshitz *et al.*, the thermal spike (stage II) has only a second-order effect, with the collision (stage I) and relaxation (stage III) stages are more effective for film evolution. A little later, Robertson and McKenzie individually proposed a modified subplantation model based on the thermal spike concept and densification[6] or compressive stress[5] induced by shallow subsurface implantation, respectively. Robertson assumes two opposite processes, i.e., the densification due to subplantation of incoming carbon species, leading to an increasing sp^3 bonding fraction as the density increases, and the second process leads to a relaxation in density toward an sp^2-bonded graphitic phase due to rearrangements occurring during a thermal spike. In McKenzie's stress model, the high local intrinsic-stress produced by subplantation of carbon species moves *a*-C into the stable domain of diamond (Berman-Simon line) in the *P-T* phase diagram of carbon[14] and thereby stabilize sp^3 bonding, and stress could release due to thermally activated relaxation processes during a thermal spike. Besides these subplantation models, a cylindrical spike model[15] and several molecular-dynamics simulation studies[16–18] of the growth of diamondlike phase have been proposed. Most of them are still based on the impact process of hyperthermal species on the target, in which some physical quantities, such as R_p and ΔR_p in subplantation process, are generally considered and introduced. Although the precise details of implantation and relaxation processes remain unclear, among the experimental and theoretical investigations, a very interesting phenomenon has been noted. That is, the ta-C film is predicted to be sp^2 bonded near the outmost surface above the depth at which subsurface conversion to the denser sp^3-bonded structure occurs.[5] McKenzie has proposed that the upper surface of ta-C film is a free surface and stress there can be relieved by the movement of surface atoms. The stress will drop from its bulk value inside the film to zero at the surface over some characteristic length, crossing the Berman-Simon line. Consequently, graphite will be the stable phase on the immediate surface. Gilkes, Gaskell, and Yuan[19] estimated an sp^2-bonded surface layer of maximum thickness 0.9 nm, by comparing the integrated area of $1s \rightarrow \pi^*$ peak in their electron energy-loss spectroscopy (EELS) of ta-C samples with different thicknesses. The estimation has been originally based on the prediction by McKenzie. Recent investigations by using spatially resolved EELS (Refs. 20 and 21) have suggested a cross-sectional structure of ta-C, in which the thickness of sp^2-bonded surface layer could be influenced by ion energy. However, the sp^2-bonded surface layer was proposed to be present during the growth of sp^3-bonded material rather than formation in the final stage of film growth induced by stress relaxation.

In recent years, great efforts have been spent upon the study of optical, mechanical, and electron-emission properties of ta-C, correlated with sp^3 content.[8,22–25] As yet, however, adequate investigation concerning the atomic structure, particularly the cross-sectional and surface structure, has not been reported. Although very thin, sp^2-bonded surface layer may play somewhat important role in either evaluating the structural and physical properties, or in actual application, e.g., application of electron emission property in vacuum microelectronics. Besides very few and sophisticated analyses by EELS, however, no direct and observable results on this issue have been reported. There exists an open question on the real structure of ta-C, which needs further investigation in order to better understand the growth process of highly tetrahedrally bonded carbon film.

In this work, we first consider that ta-C film not only exists a pretty thin sp^2-bonded surface layer, but also consists of a relatively thick sp^2-bonded carbon-rich interface between film and substrate, which could appear in the initial stage of subplantation before a pure ta-C growth. So, we can image the cross-section of ta-C as $A/B/A$ ''sandwich'' structure, where two *A* layers represent the surface and interface sp^2-bonded carbon, and *B* is the real ta-C that consists of essentially sp^3-bonded carbon. In the following sections, we will present the experimental investigation by using high-resolution transmission electron microscopy (HRTEM) in both planar and cross-sectional configurations, as well as slow positron annihilation (SPA) technique to investigate the atomic structure in surface, interior film, and interface of ta-C. Based on the subplantation model, a classical-trajectory calculation focused on the R_p and ΔR_p of hyperthermal carbon species implantation into silicon is conducted for interpreting the observed results.

II. EXPERIMENT

The ta-C films studied here were synthesized in a FAD system, which has been described in detail elsewhere.[26] Briefly, a cathodic arc discharge on a high-purity graphite cathode was used to produce a highly ionized carbon plasma. A curved magnetic-field plasma duct guides the plasma around a 90° bend in order to eliminate macroscopic and neutral particles of graphite that are also emitted by the arc. The films were deposited on different substrates at room temperature. The base pressure of vacuum system was $\sim 10^{-4}$ Pa. Deposition rate was kept at 4–5 Å/sec, which is favorable for promoting sp^3 bonding.[27]

HRTEM observation was performed using a transmission electron microscope operating at 200 kV. Two kinds of samples were deposited on different substrates. The first one was grown on Si(100) wafer with carbon ion energy of ~220 eV to thickness of 300 nm, in order to observe the profile structure of ta-C from surface to interface by cross-sectional configuration. The method that we used to prepare cross-sectional sample is a standard one that has been used by many other researchers. The preparation procedure includes mechanical dicing, thinning by mechanical polishing, and low-angle ion milling with effective cooling. The entail process is rapid and avoids problems with contamination and ion-bombardment-induced structural changes. The other was

directly deposited on copper grid at the same condition for investigating the surface structure of ta-C by planar configuration. The slow positron annihilation measurements were carried out using a positron variable-energy beam system, obtained by a Na^{22} source. The energy of the monoenergetic positron beam was varied from 0.5 to 13 keV. Details of the experimental apparatus are described elsewhere.[28] The projected range R_p and range straggling ΔR_p of hyperthermal carbon species implantation into silicon were calculated according to Lindhard-Scharff-Schiott (LSS) theory by using Thomas-Fermi stopping cross section and Ziegler-Biersack-Littmark (ZBL) formula.[29] However, varied target composition ($Si_{1-x}C_x$) from pure silicon ($x=0$) to pure carbon ($x=1$) was applied in R_p and ΔR_p calculations, which is different from the TRIM (Ref. 30) calculation by Lifshitz and co-workers[3,4] where variation of target composition was not considered, and is closer to actual situation during subplantation process.

III. RESULTS AND DISCUSSIONS

HRTEM was used to investigate the structure of ta-C. The reasons for this are twofold: (i) the presence of an sp^2-bonded surface layer, proposed by McKenzie, Muller, and Pailthorpe,[5] can be investigated directly; (ii) the intrinsic structure of ta-C in different growth regimes can be probed, giving an insight into the growth mechanism itself. HRTEM provides a two-dimensional projection of the structure and specimen areas as small as 1 nm^2 can be probed, so that differentiation of random structures from microcrystalline networks is possible.

Here, we start the structural observation from the interface between the Si substrate and film, being the same direction as film growth. As shown in Fig. 1(a), the cross-sectional image in the side of Si substrate at the interface regime consists of clearly ordered fringes of single crystalline silicon, but mixed with some random extended fringes that embedded in silicon lattice and distributed randomly in position and size. The random fringes resulted from two kinds of disordered structures. On the one hand, the lattice-disorder of silicon could be produced by radiation-damage effects of incident carbon species. As an implanted ion slows down and comes to rest, it makes many violent collisions with lattice atoms, displacing them from their lattice sites. These displaced atoms can, in turn, displace others, and the net result is the production of a highly disordered region around the path of the ions. At sufficiently high dose, these individual disordered regions may overlap, and an amorphous layer is formed. On the other hand, implanted ions can form individual carbon domains after resting in silicon matrix. By extending the implantation, quasicontinuous carbon layer could also be formed with local concentration inversely proportional to ΔR_p. As shown in Fig. 1, the destruction of silicon lattice by impingement becomes stronger along the direction of film growth (I–V), namely, original perfect silicon lattice becomes more blurred and disordered domains enlarge and increase. Due to the restriction of picture size, we show here only part of the interface. The observed thickness of the interface from perfect silicon lattice region (I) to pure carbon film (V) is almost 40 nm, rather larger than the

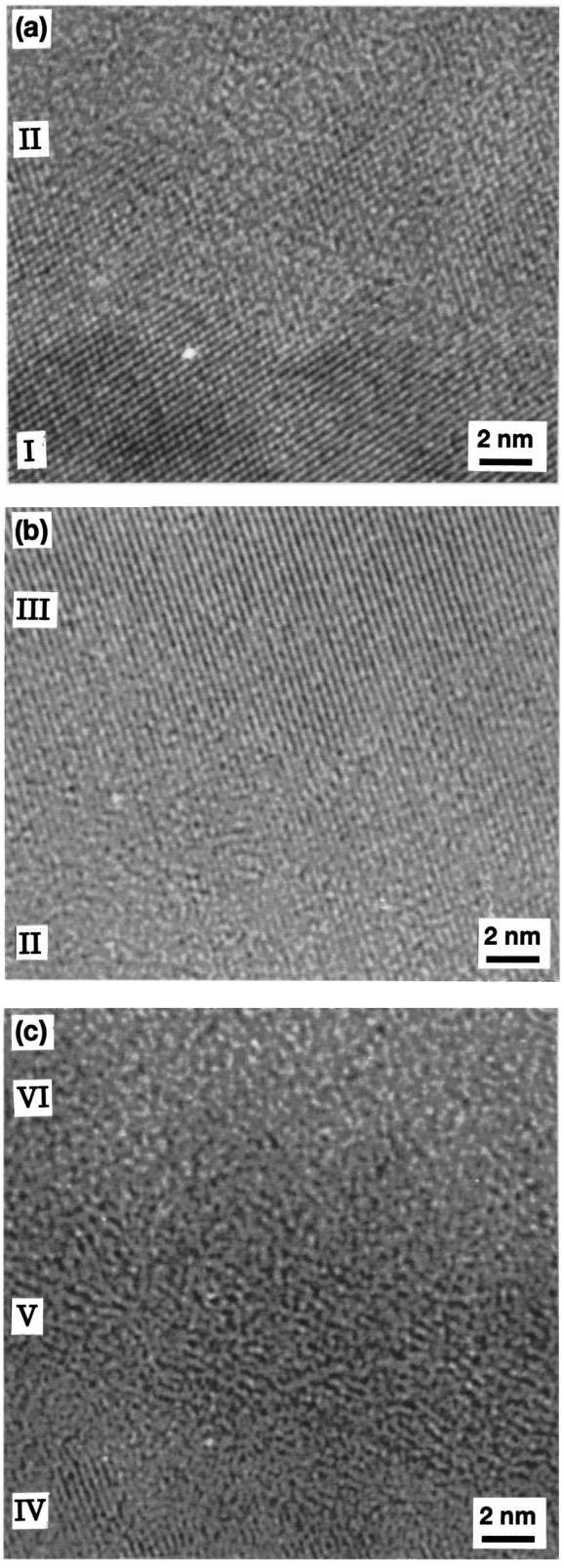

FIG. 1. Cross-sectional HRTEM image of ta-C/Si interface. (a) The side of Si substrate (I, perfect Si lattice; II, C-Si mixing layer); (b) the middle region of interface (II, C-Si mixing layer; III, low destroyed layer due to channeling); (c) the side of film (IV; the upper surface of Si substrate, V, the initial pure carbon layer; VI, the initial ta-C layer).

calculated $R_{p,}\sim 1.55$ nm, and $R_p+\Delta R_{p,}\sim 3.46$ nm, of 220 eV C^+ implantation into pure silicon target. However, it is not surprising if we consider the channeling effect (both axial and planar) that could induce the R_p to be 10 times larger or more,[31] particularly in the present case the incident C^+ beam is almost normal to the Si substrate during deposition. Recent experimental investigations[32,33] by using direct ion-beam deposition of carbon negative ions have shown an implantation depth in silicon(100) substrate to be more than 60 nm and Si-C bonding happened at the near surface of silicon substrate. If the incident C^+ enters almost parallel to a major axis or plane, then a correlated series of collisions may steer it gently through the lattice, thus reducing its rate of energy loss and increasing its penetration depth. When channeling is present, the range distribution contains two distinct components. One is the nonchanneled fraction of the incident beam, characterized by essentially the same R_p as in an amorphous target. The other is due to the channeled ions. If the dechanneling effect could be negligible, a relatively sharp distribution peak could appear at the maximum penetration range $R_{\max}$. Then, a saddle-back depth distribution of carbon species could be expected in impingement with channeling. In Fig. 1, we can distinguish two regions (II and IV) with higher concentration of carbon species on the nondamaged pure silicon matrix and below the upper surface of silicon. Between the two regions (III), carbon concentration and damage of silicon lattice are essentially lower. This saddle-back depth distribution suggests the presence of channeling during the deposition process.

Due to the damage of silicon lattice, the subsequent C^+ ions will face a nonperfect target both in chemical composition and lattice order, namely, a gradual shift of phase from one of the substrates to one of the carbon film exists through the interfacial mixing layer. Because the channeling turns out to be weak, R_p and ΔR_p will change correspondingly. The R_p and ΔR_p of 220-eV C^+ ion implantation into target with varying composition ($Si_{1-x}C_x$,$0\leqslant x\leqslant 1$) are shown in Fig. 2. Both R_p and ΔR_p reduce with carbon content, i.e., with the progressing of subplantation or film growth. An interesting phenomenon noted is that ΔR_p drops more rapidly than R_p, this means the C^+ ions have to stop at shallower layer with narrower distribution. The denser distribution of carbon species is reminiscent of the subplantation models of Lifshitz and co-workers[3,4] and Robertson.[6] The models proposed that the increased local concentration or atom density of carbon species in subsurface layer will promote the formation of sp^3 bonding. Therefore the initial carbon impingement on pure silicon target would form some carbon domains with graphitelike structure in silicon lattice due to very low local concentration or atom density. A further increase in C^+ dose due to prolonged impingement may result in a gradually increased local concentration that forms 2D carbon layer (connected graphitelike carbon domains) with some possible carbide phases, for example, silicon carbide. As shown in Fig. 1(c), carbon species with higher concentration exists at the upper surface of silicon substrate (IV). Also, it can be expected that during the early stages of subplantation, the surface is mainly composed of substrate atoms Si due to the subsurface penetration of the impinging carbon species. However, the surface silicon could be gradually sputtered and/or diluted by ion-mixing mechanisms until a surface consisting of only carbon species evolves. In Fig. 1(c), an important feature is noted in the middle area (V), that is, a pure carbon layer with distinguishable ordered structures and ~4 nm thickness is found existing in the zone just between very random upper layer (VI) and the C-Si mixing layer (IV). The fringes in this region are relatively straight and extended to form parallel layered structures, with interlayer spacing being close to 0.4 nm. Therefore, we could expect that ordered graphitic layers may occur in this region (the interlayer separation in graphite is 0.34 nm), because the layer contains only carbon materials without any observable evidence of silicon sites. This graphitelike layer with predominant sp^2 bonding could be considered as the initial layer of pure carbon film growth. After it, a pure carbon film with highly tetrahedral atomic configuration (region VI) will be formed by subsequent subplantation processes. From perfect silicon lattice (I) to the carbon-rich upper surface region (IV) in substrate, we can also expect that the observed individual carbon domains and quasicontinuous 2D carbon layers in the thick C-Si mixing region could be structurally arranged into sp^2 configuration, bearing a resemblance to the

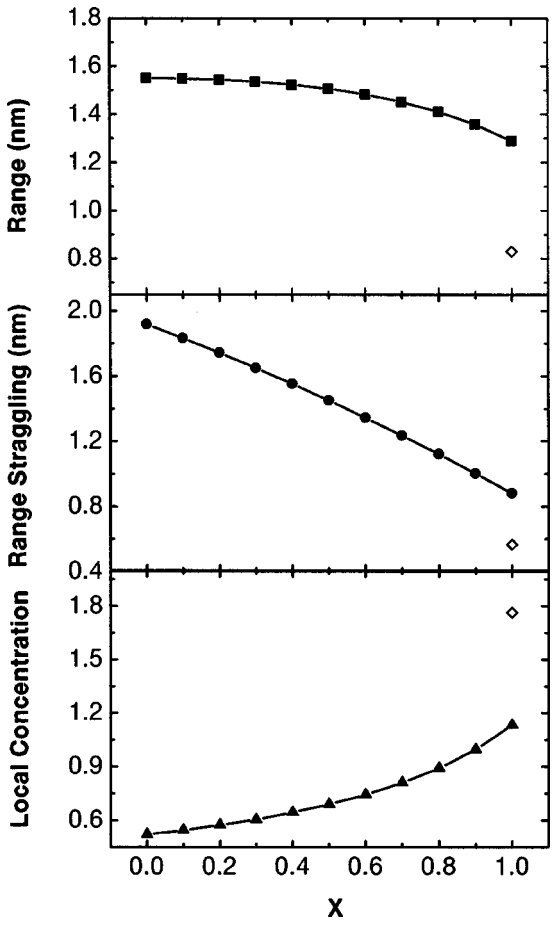

FIG. 2. Calculated (a) projected range R_p, (b) range straggling ΔR_p, and (c) local concentration ΔR_p^{-1} of 220-eV C^+ implantation into $Si_{1-x}C_x$ binary-target with varying composition ($0\leqslant x\leqslant 1$) and diamond ($\diamond$).

initially pure carbon layer (V) due to much lower local concentration of carbon species. Furthermore, it is well known that ion bombardment of a low-energy, low-mass species upon a heavier mass substrate will result in partial backscattering away from the substrate. The hyperthermal carbon species impinging on Si substrate is in this classification. Therefore, it is unlikely to attain a high, localized carbon concentration and compressive stress necessary for the creation of a high percentage of tetrahedrally coordinated C bonds when a large fraction of the incoming species is being backscattered. It will result in the interfacial mixing layer and the initially grown pure carbon layer being sp^2 bonded and having low density. As a pure carbon layer developed, however, the impinging carbon species experience increasing interaction with a growing carbon film rather than with the silicon substrate. Backscattering of carbon species decreases in frequency, allowing a film with higher density and sp^3 bonding content to grow on top of the initially pure carbon layer. Nevertheless, the possibility of sp^3-bonding formation on certain sites in the C-Si mixing layer cannot be ruled out due to occasionally increased local carbon concentration and atom density.

Based on the above discussion, we propose that the evolution of a pure carbon film from hyperthermal carbon species impinging on Si substrate consists of two subsequent deposition processes, i.e., the initial ''heterodeposition'' followed by evolution into a pure carbon film in host matrix, and the ''homodeposition'' of energetic species adding to the pure film. Target with higher carbon concentration will result in shallower implantation (R_p) and narrower distribution (ΔR_p), and therefore increase the probability of sp^3-bonding formation. Actually, as shown in Fig. 2(c), the local concentration (ΔR_p^{-1}) is found to increase with prolonging the impingement due to the evolution of target composition. Therefore, one can expect that sp^3 bonding could become favorable to sp^2 bonding by extending the deposition. While the initially pure carbon layer growth, the local concentration and atom density would reach to maximum. R_p and ΔR_p are 1.23 nm and 0.88 nm for C^+ impinging on graphite target and 0.83 nm and 0.57 nm for C^+ impinging on diamond target, respectively. In this case, diamond could be the most favorable phase to be formed and retained if there were not enough diffusion or relaxation by thermal spike or substrate heating. Thermal spike effect (stage II in the subplantation model of Lifshitz *et al.*[4]) can play a significant role in the final structure of the evolving film, mainly depending on the energy and nature of the projectile-target system. As for the substrate heating, it has been suggested that the growth temperature ($\sim$0.05 eV) has a strong effect on the processes immediately following ion implantation, despite being small compared to the ion energy.[21] That is, the enhanced atom mobility (diffusion) after subsurface implantation caused by substrate heating will prevent sp^3-bond formation and evolution. In the present study, the substrate was almost kept at ambient temperature. Therefore, obvious diffusion process could not be expected during deposition, and a diamondlike phase will be formed on the initial pure carbon layer, as shown in Fig. 1(c) (region VI). The cross-sectional image of pure ta-C film is shown in Fig. 3. The

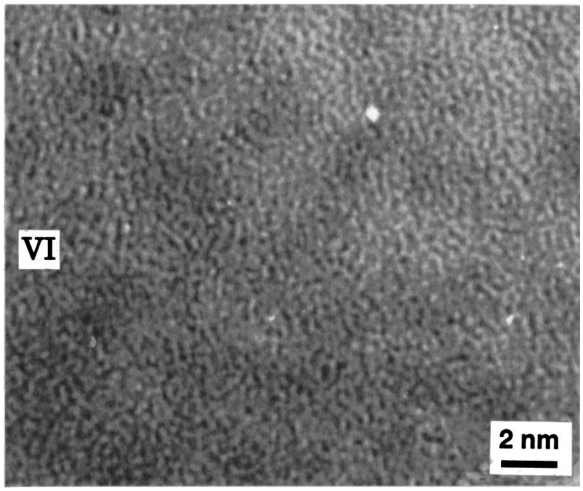

FIG. 3. Cross-sectional HRTEM image of interior film of ta-C, i.e., the pure ta-C layer.

image consists of a random background characteristic of amorphous thin film, and no distinct nonrandom features on this background are detected. The fringes are seldom straight, and extend over distances of no more than 1 nm. Moreover, it can be observed that the region is uniform in contrast and arrangement, and can be differentiated from the initially pure carbon layer (region V in Fig. 1) by image contrast and the degree of disorder. We perform an EELS analysis on this film, and results indicate the average sp^3 content to be $\sim$90%. Film density obtained by EELS and Rutherford-backscattering spectrum (RBS) is more than 3.2 g/cm^3. Electron diffraction patterns on this region exhibit broad and diffuse halos, with no evidence of microcrystallinity, both in graphite or diamond. It means that random networks of highly tetrahedrally bonded carbon phase (ta-C) was formed and evolved during subplantation process after the initially pure carbon layer growth. The compressive stress of this film determined from the substrate curvature was found to be 4.3 GPa, close to the typical value of $\sim$5 GPa found by McKenzie, Muller, and Pailthorpe.[5] Therefore, the effective hydrostatic pressure of this stress would drive the film into the diamond-stable zone as defined by the Berman-Simon curve in the *P-T* phase diagram of carbon.[14] The film thickness measured by cross-sectional observation is around 300 nm, which is consistent with the preset deposition rate (4–5 Å/sec) for 10 min deposition.

Further detailed investigations have been conducted on the near-surface region. The profile structure of this region is shown in Fig. 4. A pure Ta-C layer (VI) with the same atomic structure as that shown in Fig. 3 exists at the region below the upper surface of the film. However, carbon atoms are arranged relatively ordered in the area adjacent to the film surface (VII), with the orientation of atoms approximately paralleling the surface. The fringes in this area are relatively straight, spaced by about 0.4 nm, implying that ordered graphitelike layers occur in the surface. The ordered surface layer extends over a distance of 1–2 nm ($\sim$5 atom layers), which is consistent with the penetration depth of 220-eV carbon ions implantation into carbon target (R_p

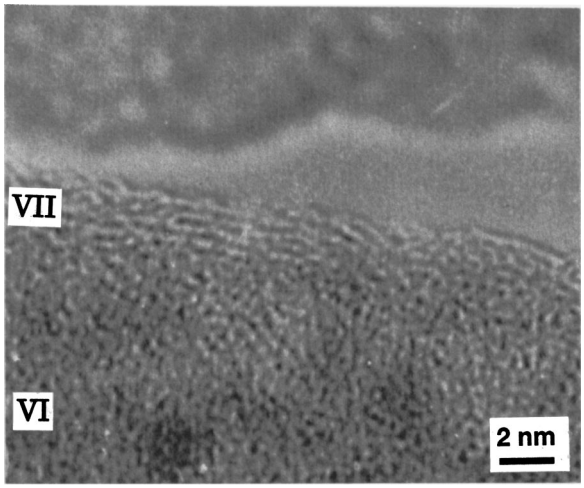

FIG. 4. Cross-sectional HRTEM image of the near-surface region in ta-C in which region VI is the interior film and region VII the upper surface layer.

$+\Delta R_p$ in diamond and graphite is around 1.4 and 2.2 nm, respectively). The fact that an sp^2-bonded surface is present in a primarily sp^3-bonded film has been predicted by McKenzie, Muller, and Pailthorpe due to the stress relaxation on a free surface.[5] Graphitelike structure will be the stable phase on the immediate surface, below it, a primarily sp^3-bonded diamondlike phase will be formed due to the increased local compressive stress produced by subplantation. Davis, Amaratunga and Knowles[21] recently proposed that the sp^2-bonded surface layer does not form after film growth due to stress relaxation,[5] but instead is present during the growth of the sp^3-bonded material. That is, as film grows, the bottom part of an initially sp^2-bonded layer is converted to sp^3 bonding by a subsurface deposition process due to subplantation, and the top layer expands away from the substrate to form final sp^2-bonded surface layer. However, it should be noted that one important physical quantity included in subplantation model by Lifshitz *et al.* is the sputtering effect.[4] The surface features of the evolving film and the efficiency of the deposition process depend on the sputtering yield (S) of both substrate and trapped atoms by the impinging ions. Although ion energy is not so high, the C^+ fluence used in FAD process is large enough. One weakly bonded graphite-like top layer could be easily sputtered or displaced inside by knock-on collisions. Because the self-sputtering coefficient of carbon is less than 1 for all ion energies, however, a few sp^2 bonds formed during the film growth should retain in the surface region. Considering the surface stress relaxation proposed by McKenzie, Muller, and Pailthorpe,[5] the sp^2 bonds in the surface region should develop further and an ordered sp^2-bonded surface layer would form immediately while stopping deposition, i.e., in the final stage of film growth.

More detailed investigation is therefore necessary for characterizing the surface carbon configuration in ta-C. It is of special significance in both fundamental and practical aspects. It could serve as a direct evidence of subplantation model for film growth from hyperthermal species, especially for sp^3-bonded material. It is also relevant to correctly perform analysis of structural measurements that could be affected by the entire film, such as EELS, Raman spectroscopy, x-ray diffraction, and so on. In the practical aspect, a typical example is the study and application of its excellent field-emission property,[24,25] because an sp^2-bonded surface layer might play an important role in electron-emission process. We will discuss this situation in detail after characterizing the surface arrangement of carbon atoms.

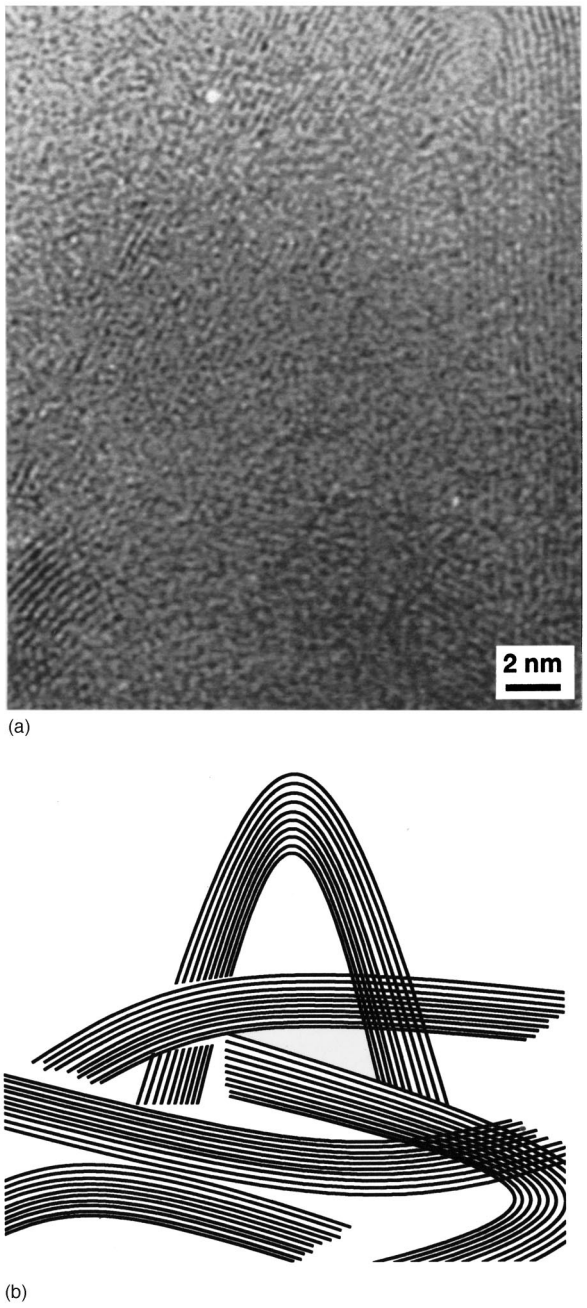

FIG. 5. (a) Planar HRTEM image of the atomic configuration in ta-C surface; (b) the schematic illustration of the entangled ribbons.

For this purpose, ta-C film was directly deposited onto copper grid for HRTEM observation without any thinning process, for example, polishing and ion milling. A typical image is shown in Fig. 5. Two different regions could be

distinguished based on the degree of order in atomic configurations. Besides some disordered regions where carbon atoms are arranged randomly, a large number of ordered layer structures exists in the manner of entangled ribbons that is similar to that of glassy carbon, and some sites are found to be highly strained. It is well known that the most ordered form of synthetic graphite is called highly oriented pyrolytic graphite, and is produced by heat and pressure treatments up to 3500 °C.[34] The d spacing of pyrolytic graphite is around 0.34 nm. Franklin noted that pyrolytic carbon could be classified as being either graphitizing or nongraphitizing, according to whether the graphitization occurred during heating.[35] Nongraphitizing carbon, which is called glassy carbon later, consists of an ordered and a disordered component, and that parallel layers in ordered region develop with much more difficulty, only (002) interlayer peak of graphite lattice can be observed by diffraction.[35,36] Two ''correlation lengths'' have been defined to describe the structure of glassy carbon,[37] in which L_a is a length over which a layer is flat, and L_c corresponds to the distance over which layers are parallel. Franklin concluded that 65% of the atoms in glassy carbon were in turbostatic graphitic domains, with the remainder in disordered regions of unspecified character[36]. Although Noda, Inagaki, and Yamada[38] suggested that glassy carbon may contain a proportion of sp^3 sites, Mildner and Carpenter[39] concluded that no evidence for any sp^3 sites existed in glassy carbon. Based on these results, therefore we could point out that the surface layer of ta-C, as shown in Figs. 4 and 5, will take on the structural configuration of a glassy carbon after stress relaxation, which is considerably different from that of evaporated a-C, a much more disordered form of carbon with dominant sp^2 bonding. This partially or relatively ordered surface carbon consists of strained parallel layers stacked in a disordered manner. From Fig. 5 we can know that the two ''correlation lengths'' L_a and L_c in the sample are around 12 nm and 4–6 nm, respectively, which agree well with the values of glassy carbon obtained by Jenkins and Kawamura.[40] The spacing between parallel layers is ~0.36 nm, approaching the interlayer spacing of glassy carbon ($d=0.37$ nm) (Ref. 36) and a little larger than that of perfect graphite ($d=0.34$ nm). The increased interlayer spacing might be induced by the relative disorder. A schematic illustration of the entangled ribbons of glassy carbon is shown in Fig. 5(b). Electron diffraction from the planar TEM sample shows a relatively strong but diffuse (002) halo, implying a layered graphitic structure, although with disordered layer stacking. The presence of diffuse (002) reflections is consistent with most of the diffraction investigations on glassy carbon, in which only (002) interlayer peak was observed.[36,37] That is, due to compressive stress relaxation, not only is sp^3 converted to sp^2 bonding, but the resulting sp^2-bonded surface layer shows substantially much longer range order than evaporated a-C, in which the majority of carbon sites have sp^2 bonding. Furthermore, the presence of ordered sp^2-bonded structure revealed by both cross-sectional and planar observations suggests that the film experienced very high local temperature during deposition, which was induced by thermal spike during subplantation of hyperthermal carbon species.

So far, the cross-sectional and planar atomic structures of ta-C films have been discussed in detail based on the HRTEM observations. As shown in Fig. 3, a basic structural contour could be imaged as sandwiched multilayers with $A/B/A$ stacks, in which two A layers stand for the sp^2-bonded thick interface and thin surface, and B layer represents the real ta-C which is essentially sp^3 bonded. Note that in most structural analyses in literature,[2,8,41,42] EELS is used to give a quantitative ratio of sp^3 to sp^2 bonding in ta-C films. However, these analyses have assumed that ta-C films are homogeneous in structure and bonding state. HRTEM observation indicates that this is not the case. Based on the above results, we could, therefore, conclude that the fraction of sp^3 sites in the interior of ta-C film must be higher than those reported values determined by EELS calculation. The interior sp^3 content and atomic density should be very close to those of diamond, if the film has been synthesized at optimum C^+ ion energy and flux. Therefore, ta-C could be referred to as the amorphous form of diamond, structurally similar to a-Ge and a-Si that are positioned in the same group as carbon in the Periodic Table. Due to the existence of sp^2-bonded interface and surface layer, we could also conclude that it is impossible to synthesize fully the sp^3-bonded ta-C. That is, the presence of sp^2 bonding seems to be an intrinsic property of ta-C.

Further investigation on the structure of ta-C is carried out using SPA. SPA is one of the most powerful methods to study the structural disorder caused by ion implantation. However, the interpretation of SPA resulting from amorphous carbon is not straightforward, due to the complexity of the systems. Until now only a few SPA studies on disordered carbon films have been done.[43–45] For ta-C, as yet, no reported data is available. As most of SPA studies, the shape parameter S is used to characterize the Doppler-broadened 511-keV annihilation gamma line. The S parameter increases when the positrons annihilate in open volumes, namely, more dense phase exhibits more low S parameters. In present study, experimental S parameter is simulated by assuming that the annihilation of incident variable-energy positrons could take place at the surface (S_s), interior film (S_i), interface (S_f) and Si substrate (S_{Si}), respectively. The fitting results of the S parameter indicate $S_s(0.4949)$ and $S_f(0.4779)$ are relatively larger than $S_i(0.4468)$. It could imply that the interior film might possess much higher compactiveness than the surface and interface regions. The results are in good agreement with those obtained from HRTEM observation, i.e., highly tetrahedrally bonded interior film are much denser than graphitic surface and interface. Although SPA is not able to give a direct and completely accepted argument, it is of significance as a circumstantial evidence for HRTEM results.

The above results based on HRTEM and SPA investigations indicate a very interesting phenomenon, that is, ta-C deposited by hyperthermal carbon species should have a sandwich $A/B/A$ stacking structure (see Fig. 6). The existence of such a structure will be a powerful evidence for subplantation model and compressive-stress mechanism for

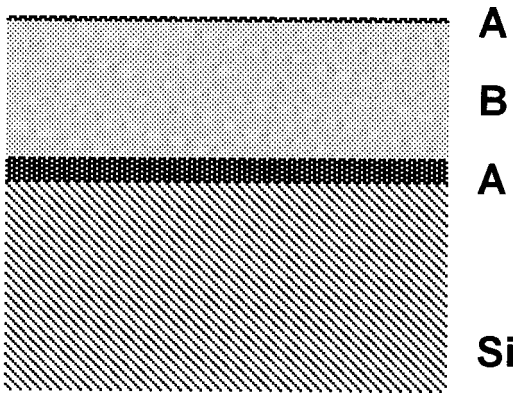

FIG. 6. Schematic illustration of sandwich structure with $A/B/A$ stacks, in which the bottom A stands for the thicker sp^2-bonded interface, the top A is the thinner sp^2-bonded surface, and B is the sp^3-bonded interior layer of ta-C.

sp^3 phase evolution suggested by Lifshitz and co-workers,[3,4] Robertson,[6] and McKenzie, Muller, and Pailthorpe,[5] respectively. Such a structure also possesses potential value in actual application of ta-C. For example, ta-C has been extensively investigated on electron-field-emission property. Almost all the reported emission data have been interpreted based on the premise that ta-C is a uniform amorphous semiconductor both in structure and bonding state with high fraction of sp^3 bonds. However, according to the present results, it could be expected that the thin sp^2-bonded surface layer might play an important role in electron emission process. An sp^2-bonded layer can easily serve as a source to supply electron to emit, especially when a layer-by-layer deposited ta-C will be performed on field-emission measurement. In such multilayer structure, as shown in Fig. 7 schematically, graphitic sp^2-bonded layer A can eject electrons to semiconducting sp^3-bonded layer B, then the sp^3 layer could easily

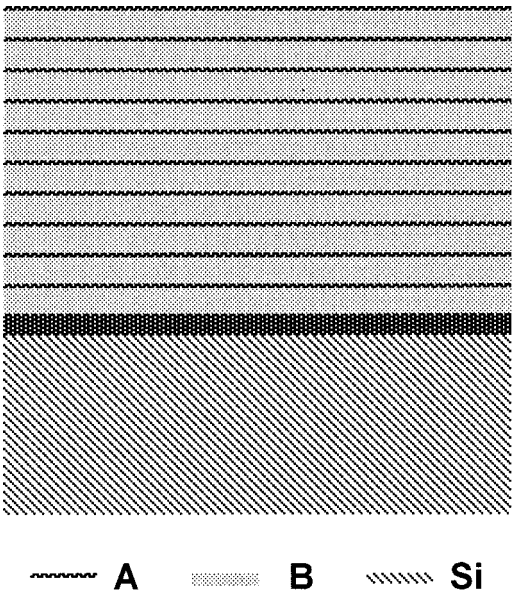

FIG. 7. Schematic illustration of layer-by-layer deposited ta-C multilayers with $A/B/A/B/\ldots/A/B/A$ stacks.

emit electrons into vacuum due to its wide bandgap and low emission barrier.[24] The electron emission property, therefore, could be easily modulated by changing the total layer number and the thickness per layer. We would note that the actual experimental investigations on this assumption have already been completed,[46] with the results agreeing well with those expected.

IV. CONCLUSIONS

ta-C films have performed detailed cross-sectional and planar HRTEM investigations for the atomic structures at surface, interior film, and interface between film and substrate, respectively. A few significant results were obtained and further confirmed by ion range calculation and SPA analysis.

(1) The cross-sectional HRTEM images revealed that a sandwich structure should exist in ta-C film and can be expressed as $A/B/A$ layer-by-layer stacks. That is, the first A layer is a very thin (1–2 nm) sp^2-bonded surface with a structure characteristic of glassy carbon, B represents the real tetrahedrally bonded carbon interior film, and the other A is a thick ($\sim$40 nm) sp^2-bonded interface with possible $Si_{1-x}C_x$ inclusions.

(2) The much thicker interface than the calculated $R_p + \Delta R_p$ is probably induced by channeling effect of hyperthermal carbon species implantation. By comparing the projected range (R_p) and local concentration (ΔR_p^{-1}) of carbon species implantation into $Si_{1-x}C_x$ binary target with variable composition ($0 \leqslant x \leqslant 1$), it can be expected that sp^3-bonded structure will be the most favorable phase to form while a pure carbon layer or phase appears.

(3) Planar view of ta-C surface structure indicated that besides some disordered sites, a large number of ordered structure existed in the surface area of ta-C, in the manner of entangled ribbons that were identified to be sp^2-bonded glassy carbon with some sites being highly strained. Electron diffraction and interlayer spacing of 0.36 nm have supported the identification. The atomic arrangement in the surface area of ta-C are substantially different from that of evaporated a-C.

(4) SPA provides circumstantial evidence for HRTEM results. The higher S parameter at the surface and the interface as compared to the interior film implied that the interior layer of ta-C is more compactive than the surface and interface.

(5) The content of sp^3 sites in the interior of ta-C film must be higher than those reported values in literatures calculated by EELS, according to the present investigations. The ordered sp^2-bonded surface layer should be formed immediately while stopping deposition due to the relaxation of surface stress, i.e., formation in the final stage of subplantation.

(6) The sandwich structure is of significance in both fundamental and application aspects. It gives a powerful and direct corroboration of subplantation model for film growth from hyperthermal species, suggested by Lifshitz and Robertson, respectively, and the compressive stress mechanism

for sp^3 sites evolution proposed by McKenzie. It is of clear importance to correctly perform analysis of structural measurements and to better understand the properties of ta-C that could be highly dependent on the existence of sp^2-bonded interface and surface. It also possesses potential values in actual application, for example, in electron-field emission from ta-C.

ACKNOWLEDGMENTS

The material is based on work supported by the National Hi-Tech R&D project of China. The authors would like to express their gratitude to JST and NEDO, Japan, for financial support. Professor W. I. Milne of University of Cambridge is gratefully acknowledged for valuable discussion.

*Corresponding author. FAX: +81-87-869-3551. Electronic address: zhao@sniri.go.jp

[1] S. D. Berger, D. R. McKenzie, and P. J. Martin, Philos. Mag. Lett. **57**, 285 (1988).
[2] P. H. Gaskell, A. Saeed, P. Chieux, and D. R. McKenzie, Phys. Rev. Lett. **67**, 1286 (1991).
[3] Y. Lifshitz, S. R. Kasi, and J. W. Rabalais, Phys. Rev. Lett. **62**, 1290 (1989).
[4] Y. Lifshitz, S. R. Kasi, J. W. Rabalais, and W. Eckstein, Phys. Rev. B **41**, 10 468 (1990).
[5] D. R. McKenzie, D. A. Muller, and B. A. Pailthorpe, Phys. Rev. Lett. **67**, 773 (1991).
[6] J. Robertson, Philos. Trans. R. Soc. London, Ser. A **342**, 277 (1993).
[7] Y. Lifshitz, G. D. Lempert, and E. Grossman, Phys. Rev. Lett. **72**, 2753 (1994).
[8] P. J. Fallon, V. S. Veerasamy, C. A. Davis, J. Robertson, G. A. J. Amaratunga, W. I. Milne, and J. Koskinen, Phys. Rev. B **48**, 4777 (1993).
[9] G. M. Pharr, D. L. Callahan, D. McAdams, T. Y. Tsui, S. Anders, A. Anders, J. W. Ager III, I. G. Brown, C. Singh Bhatia, S. R. P. Silva, and J. Robertson, Appl. Phys. Lett. **68**, 779 (1996).
[10] E. Grossman, G. D. Lempert, J. Kulik, D. Marton, J. W. Rabalais, and Y. Lifshitz, Appl. Phys. Lett. **68**, 1214 (1996).
[11] C. Weissmantel, in *Thin Films From Free Atoms and Particles*, edited by K. J. Klabunde (Academic, Orlando, FL, 1985), Chap. 4.
[12] S. Uhlmann, Ph.D. thesis, University Chemnitz, 1997.
[13] J. Koike, D. M. Parkin, and T. E. Mitchell, Appl. Phys. Lett. **60**, 1450 (1992).
[14] R. Berman and F. Simon, Z. Elektrochem **59**, 333 (1955).
[15] H. Hofsäss, H. Feldermann, R. Merk, M. Sebastian, and C. Ronning, Appl. Phys. A: Mater. Sci. Process. **A66**, 153 (1998).
[16] N. A. Marks, D. R. McKenzie, and B. A. Pailthorpe, Phys. Rev. B **53**, 4117 (1996).
[17] N. A. Marks, D. R. McKenzie, B. A. Pailthorpe, M. Bernasconi, and M. Parinello, Phys. Rev. B **54**, 9703 (1996).
[18] H. P. Kaukonen and R. M. Nieminen, Phys. Rev. Lett. **68**, 620 (1992).
[19] K. W. R. Gilkes, P. H. Gaskell, and J. Yuan, J. Non-Cryst. Solids **164-166**, 1107 (1993).
[20] C. A. Davis, K. M. Knowles, and G. A. J. Amaratunga, Surf. Coat. Technol. **76-77**, 316 (1995).
[21] C. A. Davis, G. A. J. Amaratunga, and K. M. Knowles, Phys. Rev. Lett. **80**, 3280 (1998).
[22] M. Chhowalla, Y. Yin, G. A. J. Amaratunga, D. R. McKenzie, and Th. Frauenheim, Appl. Phys. Lett. **69**, 2344 (1996).
[23] M. Chhowalla, J. Robertson, C. W. Chen, S. R. P. Silva, C. A. Davis, G. A. J. Amaratunga, and W. I. Milne, J. Appl. Phys. **81**, 139 (1997).
[24] J. Robertson, Thin Solid Films **296**, 61 (1997).
[25] L. K. Cheah, X. Shi, E. Liu, and B. K. Tay, J. Appl. Phys. **85**, 6816 (1999).
[26] J. P. Zhao, X. Wang, Z. Y. Chen, S. Q. Yang, T. S. Shi, and X. H. Liu, J. Phys. D **30**, 5 (1997).
[27] Z. Y. Chen, Y. H. YU, J. P. Zhao, X. Wang, X. H. Liu, and T. S. Shi, J. Appl. Phys. **83**, 1281 (1998).
[28] D. Z. Wang, H. M. Weng, and J. L. Yang, J. Funct. Mater. **26**, 643 (1995).
[29] J. F. Ziegler, J. P. Biersack, and U. Littmark, *The Stopping and Ranges of Ions in Matter* (Pergamon, Oxford, 1985), Vol. 1.
[30] J. P. Biersack and W. Eckstein, Appl. Phys. A: Solids Surf. **A34**, 73 (1984).
[31] G. Dearnaley, J. H. Freeman, G. A. Gard, and M. A. Wilkins, Can. J. Phys. **46**, 587 (1968).
[32] M. H. Sohn, S. I. Kim, and K. Siangchaew, J. Mater. Res. **14**, 3221 (1999).
[33] M. H. Sohn and S. I. Kim, J. Mater. Res. **14**, 2668 (1999).
[34] A. W. Moore, in *Physics and Chemistry of Carbon*, edited by P. L. Walker (Dekker, New York, 1973), Vol. 11.
[35] R. E. Franklin, Proc. R. Soc. London, Ser. A **209**, 196 (1951).
[36] R. E. Franklin, Acta Crystallogr. **3**, 107 (1950).
[37] G. M. Jenkins, K. Kawamura, and L. Ban, Proc. R. Soc. London, Ser. A **327**, 501 (1972).
[38] T. Noda, M. Inagaki, and Y. Yamada, J. Non-Cryst. Solids **1**, 285 (1969).
[39] D. F. R. Mildner and J. M. Carpenter, J. Non-Cryst. Solids **47**, 391 (1982).
[40] G. M. Jenkins and K. Kawamura, *Polymeric Carbons* (Cambridge University Press, Cambridge, 1976).
[41] J. Kulik, Y. Lifshitz, G. D. Lempert, J. W. Rabalais, and D. Marton, J. Appl. Phys. **76**, 5063 (1994).
[42] D. L. Pappas, D. L. Saenger, J. Bruley, W. Krakow, J. J. Cuomo, T. Gu, and R. W. Cdlins, J. Appl. Phys. **71**, 5675 (1995).
[43] G. Kögel, D. Schödlbauer, W. Triftshäuser, and J. Winter, Phys. Rev. Lett. **60**, 1550 (1988).
[44] F. L. Freire, Jr., C. A. Achete, R. S. Brusa, G. Mariotto, X. T. Teng, and A. Zecca, Solid State Commun. **91**, 965 (1994).
[45] F. L. Freire, Jr., D. F. Franceschin, R. S. Brusa, G. R. Karwasz, G. Mariotto, A. Zecca, and C. A. Achete, J. Appl. Phys. **81**, 2451 (1997).
[46] J. P. Zhao, Z. Y. Chen, X. Wang, and T. S. Shi, J. Appl. Phys. **87**, 8098 (2000).